Conductance of a double quantum dot system in the Kondo regime in the presence of inter-dot coupling and channel mixing effects

2007 J. Phys.: Condens. Matter 19 256205

(http://iopscience.iop.org/0953-8984/19/25/256205)

IOP PUBLISHING JOURNAL OF PHYSICS: CONDENSED MATTER

J. Phys.: Condens. Matter **19** (2007) 256205 (15pp) doi:10.1088/0953-8984/19/25/256205

Conductance of a double quantum dot system in the Kondo regime in the presence of inter-dot coupling and channel mixing effects

D Sztenkiel and R Świrkowicz

Faculty of Physics, Warsaw University of Technology, ulica Koszykowa 75, 00-662 Warsaw, Poland

E-mail: DSZ@poczta.fm

Received 21 March 2007, in final form 7 May 2007
Published 5 June 2007
Online at stacks.iop.org/JPhysCM/19/256205

Abstract

Electron transport through a parallel double quantum dot is theoretically studied in the Kondo regime with the use of the non-equilibrium Green function formalism based on the equation of motion method. An influence of inter-dot tunnel coupling t and channel mixing effects on the orbital (spinless) Kondo phenomenon is analysed in the linear and nonlinear transport regimes. Both effects lead to a considerable suppression of the conductance in the Kondo regime. In a system with dots capacitively coupled ($t = 0$) the differential conductance shows a zero-bias peak whose intensity diminishes gradually with mixing effects included. When tunnel coupling between dots is taken into account ($t \neq 0$) the orbital Kondo resonance splits and the intensities of both components are strongly influenced by channel mixing. The linear conductance calculated as a function of a dot level position E_0 is strongly suppressed in the Kondo regime but at higher values of E_0 a relatively well-pronounced side peak appears whose intensity increases with the coupling rate t. We consider the side peak maximum as originated from interference processes in the system.

1. Introduction

Electronic transport through a double quantum dot (DQD) system has attracted much research interest in recent years due to the possibility of using such systems in quantum computation [1, 2]. At low temperatures, a DQD reveals a broad variety of transport regimes, such as the Kondo effect in dots strongly coupled to external leads [3–6], Fano resonance [4, 7] or Aharonov–Bohm oscillations [8, 9]. Fano resonance arises from quantum interferences between two different paths accessible for electrons during tunnelling through the system, and it has been observed in a variety of experiments [4, 7, 10] as well as having been studied

theoretically by means of various techniques [11, 12]. The interplay between Fano and Kondo resonances has also been investigated [13–15]. A strong suppression of the conductance in the Kondo regime due to destructive interference processes was obtained [13, 16].

The ordinary Kondo phenomenon manifests itself in a considerable enhancement of the linear and nonlinear conductance and arises from spin fluctuations [17]. The observation of the spin Kondo effect in an artificial quantum dot molecule was reported by Jeong *et al* [18]. A splitting of the Kondo resonance due to an energy difference between two molecular states formed by the coherent superposition of the Kondo effects of each dot was obtained. The splitting was also predicted by theoretical studies performed for two dots in a series in a limit of strong inter-dot coupling t [19, 20]. On the other hand, in a system with weak coupling the Kondo resonance is formed between each dot and the corresponding lead, and no splitting of the anomaly was observed [19, 21]. The competition between the Kondo effect and antiferromagnetic coupling generated via exchange or via capacitive coupling between two dots has also been studied [19, 22].

The existence of a degenerate ground state is a fundamental element of a system for the Kondo effect to develop. Most commonly, the phenomenon arises from a two-fold spin degeneracy, but in a general case the spin degree of freedom can be replaced by any, two-valued, quantum number. Moreover, systems with N-degenerated ground states can exhibit various Kondo effects depending on the allowed transitions between the degenerated states [23]. An interplay between orbital and spin degrees of freedom can lead to the Kondo phenomenon with $SU(4)$ symmetry. Such a highly symmetric Kondo effect was observed in carbon nanotubes [24] as well as in vertical semiconductor QDs [25]. Nanotubes show an intrinsic orbital degeneracy which corresponds to two ways in which electrons can circle around the graphene cylinder, namely clockwise or counterclockwise. In the case of vertical QDs, orbitals correspond to two degenerate Fock–Darwin states with different values of angular momentum quantum number. Theoretical approaches to $SU(4)$ Kondo physics were undertaken by several authors and a variety of techniques was employed [26–35]. It is worth mentioning that the Kondo temperature of the $SU(4)$ effect $T_{\mathrm{K}}^{SU(4)}$ is in general at least one order of magnitude higher than in the case of the common spin Kondo effect in QDs [31]. A transition from $SU(4)$ to $SU(2)$ Kondo effect due to symmetry breaking (e.g. by orbital anisotropy) has also been discussed in relation to carbon nanotubes [32] or DQD structures [33]. Recently, the observation of a purely orbital (spinless) Kondo anomaly in a carbon nanotube QD has been reported [36]. The effect can be observed in an external magnetic field when orbital level-crossing is attained.

The orbital Kondo resonance was observed for the first time by Wilhelm *et al* in a DQD system with each dot connected to a separate set of external electrodes and no tunnelling between dots [37]. Two degenerate states of the DQD then play the role of pseudo-spin with up and down pseudo-spins related to an extra electron in dot 1 (up) or an extra electron in dot 2 (down). When each dot is coupled to a separate set of reservoirs, processes in which an electron tunnels from dot 1 to the corresponding electrode while another electron simultaneously tunnels onto dot 2 lead to the orbital Kondo effect.

Experimental investigations of the pseudo-spin Kondo anomaly in DQDs coupled in parallel as well as a theoretical analysis of the problem were performed by Holleitner *et al* [38]. A competition between the Kondo phenomenon and molecular states was studied. As the tunnelling coupling between dots lifts the orbital degeneracy the Kondo peak is split and the anomaly is suppressed considerably for greater values of t [38]. The behaviour is similar to a suppression of the spin Kondo effect under external magnetic field [39, 40]. A finite bias singlet–triplet Kondo phenomenon in a carbon nanotube QD was experimentally investigated by Paaske *et al*, and a considerable splitting with highly asymmetric peaks was observed in the

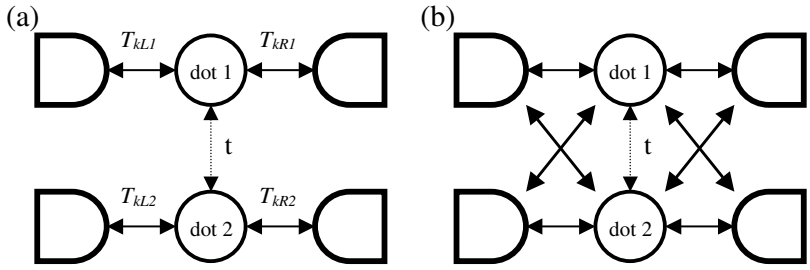

Figure 1. The schematic diagram of the system.

differential conductance [41]. A model based on a two-orbital Anderson impurity occupied by two electrons allowed the authors to describe the results obtained.

The orbital Kondo effect in DQD structures in parallel configuration with two dots capacitively coupled has been studied theoretically [42, 43]. Transport through DQDs connected in series has also been analysed [44]. In this last case the geometry ensures that each dot is coupled to its own separate electrode and the orbital quantum number is conserved. However, in parallel geometry some cross-coupling effects could take place and the conservation of orbital quantum number would be violated, so a suppression of the orbital Kondo phenomenon can be expected [33, 45].

In the present approach we analyse in detail the influence of channel mixing effects as well as inter-dot tunnelling coupling on the linear and nonlinear transport in the Kondo regime. Only the orbital Kondo effect induced by inter-dot Coulomb correlations is discussed. In the presence of strong inter-dot Coulomb repulsion one electron can be accumulated in the DQD system and fluctuations of pseudo-spin corresponding to states with an extra electron in dot 1 or dot 2 will lead to the orbital Kondo anomaly. Calculations performed in [32] show that channel mixing effects practically do not influence the spin Kondo phenomenon. As the inter-dot tunnel coupling is very weak, much weaker than coupling to the leads, one can expect that under such circumstances the spin Kondo anomaly will not be disturbed considerably. In particular, no splitting of the spin Kondo resonance was predicted for two QDs in the serial configuration with weak inter-dot coupling [19, 21], and a well-defined zero-bias Kondo anomaly was found in the differential conductance [21]. Therefore, in the present study, limited to a weak inter-dot coupling regime, we do not take into account spin degrees of freedom, and we focus only on the orbital Kondo effect. The non-equilibrium Green function technique based on the equation of motion (EOM) method is employed. A schematic diagram of the system consisting of two equivalent single-level quantum dots coupled to external reservoirs is presented in figure 1. When each dot is attached to a separate set of electrodes with no mixing between two channels the orbital quantum number is conserved during tunnelling processes and the orbital Kondo effect occurs. With channel mixing included an electron can tunnel coherently from one dot via the reservoirs to another dot. The maximal cross coupling is achieved if the quantum dots are attached to a single common lead, and this corresponds to the parallel arrangement of the dots. It is worth mentioning that the case with a finite amount of mixing to some extent relates to a quantum dot coupled to ferromagnetic leads with non-collinear magnetization directions [32, 46–48].

2. Model and Green function formalism

The two-impurity Anderson model is used to describe the system under consideration. The Hamiltonian can be written as

$$H = H_{\mathrm{L}} + H_{\mathrm{R}} + H_{\mathrm{DQD}} + H_T. \tag{1}$$

Here H_β with $\beta = \mathrm{L}, \mathrm{R}$ is the Hamiltonian for non-interacting electrons in the left ($\beta = \mathrm{L}$) and the right ($\beta = \mathrm{R}$) leads and is given by $H_\beta = \sum_k \varepsilon_{k\beta} a^+_{k\beta} a_{k\beta}$. Here $a^+_{k\beta}(a_{k\beta})$ denotes the creation (annihilation) operator of an electron of momentum k and single-particle energy $\varepsilon_{k\beta}$ in the lead β.

The term H_{DQD} describes the two-dot region and is taken in the form

$$H_{\mathrm{DQD}} = \sum_{i=1,2} E_i d_i^+ d_i + t(d_1^+ d_2 + d_2^+ d_1) + U d_1^+ d_1 d_2^+ d_2 \tag{2}$$

where E_i corresponds to the energy level of dot i, $d_i^+(d_i)$ denotes the creation (annihilation) operator of an electron in the dot i and t is the coupling between dots. The last term in Hamiltonian (2) describes the inter-dot Coulomb interaction between electrons. In this work we consider only empty or singly occupied states in each quantum dot and neglect in the Hamiltonian the term describing on-site Coulomb correlations.

The term H_T in equation (1) corresponds to the coupling between the double quantum dot region and the electrodes, and it is written as

$$H_T = \sum_{\substack{k,i=1,2 \\ \beta=L,R}} (T_{k\beta i} a^+_{k\beta} d_i + T^*_{k\beta i} d_i^+ a_{k\beta}) \tag{3}$$

with $T_{k\beta i}$ describing tunnelling of an electron from the dot i to the electrode β.

The current flowing through the system from the lead β is determined by the formula derived by Meir [49]:

$$I^\beta = \mathrm{i}\frac{2e}{\hbar}\,\mathrm{Tr}\int \frac{\mathrm{d}\varepsilon}{2\pi}\hat{\Gamma}^\beta(\varepsilon)\{\hat{G}^<(\varepsilon) + f_\beta(\varepsilon)[\hat{G}^{\mathrm{r}}(\varepsilon) - \hat{G}^{\mathrm{a}}(\varepsilon)]\} \tag{4}$$

where $f_\beta(\varepsilon)$ denotes the Fermi–Dirac distribution function for the lead β, and $\hat{G}^{\mathrm{r}}$ and $\hat{G}^{\mathrm{a}}$ stand for the Fourier transforms of retarded and advanced Green functions (GFs), whereas $\hat{G}^<$ represents the lesser one. The appropriate matrices are determined in a two-dimensional pseudo-spin space. Terms $\Gamma^\beta_{ii'}(i, i' = 1, 2)$ describe tunnelling rates and are defined by $\Gamma^\beta_{ii'}(\varepsilon) = 2\pi \sum_k T_{k\beta i} T^*_{k\beta i'} \delta(\varepsilon - \varepsilon_{k\beta})$. In the present approach the $\Gamma^\beta_{ii'}(\varepsilon)$ are assumed to be independent of energy, constant within the electron band and zero otherwise. Non-diagonal elements Γ^β_{i-i} describe mixing effects between two orbital channels. The mixing is characterized by the parameter $\alpha = \Gamma^\beta_{i-i}/\Gamma^\beta_{ii}$. $\alpha = 0$ corresponds to the case with no cross-coupling effects present in the system, whereas for $\alpha = 1$ both dots are coupled to common reservoirs and maximal mixing takes place.

In order to find retarded and advanced GFs the equation of motion method is employed. The method generates higher-order functions, which can be calculated only approximately. Considering temperatures comparable to the Kondo temperature we decouple high-order GFs using the procedure proposed by Meir [49]. The approach allows one to describe the Kondo effect in a proper way in this temperature region [50]. After these approximations are introduced and in the limit of infinite U we can write the GF in the following matrix form which corresponds to the Dyson equation (for details of calculations see the appendix)

$$\hat{G}(\varepsilon) = [\hat{g}(\varepsilon)^{-1} - \hat{\Sigma}(\varepsilon)]^{-1} \tag{5}$$

with $g_{ii'} = \delta_{ii'}(\varepsilon - E_i)^{-1}$ describing the GF of the uncoupled double quantum dot in the absence of any interaction. The term $\hat{\Sigma}(\varepsilon)$ denotes the self-energy of interacting system and is given by

$$\hat{\Sigma}(\varepsilon) = \hat{g}(\varepsilon)^{-1} - \hat{\tilde{n}}^{-1}\hat{g}(\varepsilon)^{-1} + \hat{\tilde{n}}^{-1}(\hat{\Sigma}_0 + \hat{\tilde{\Sigma}}(\varepsilon) + \hat{T}) \tag{6}$$

where $\hat{\Sigma}_0$ describes the self-energy of the non-interacting system, $T_{ii'} = \delta_{i-i'}t$, $\tilde{n}_{ii} = 1 - \langle d^+_{-i}d_{-i}\rangle$, $\tilde{n}_{i-i} = \langle d^+_{-i}d_i\rangle$ and

$$\tilde{\Sigma}_{ii}(\varepsilon) = \sum_{k,\beta} \frac{\left|T_{k\beta-i}\right|^2}{\varepsilon - \varepsilon_{k\beta}} f_\beta(\varepsilon_{k\beta}) + \sum_{k,\beta} \frac{2t^2\left(\left|T_{k\beta i}\right|^2 + \left|T_{k\beta-i}\right|^2\right)}{(\varepsilon - \varepsilon_{k\beta})[(\varepsilon - \varepsilon_{k\beta})^2 - 4t^2]} f_\beta(\varepsilon_{k\beta}) - \sum_{k,\beta} \frac{2tT^*_{k\beta i}T_{k\beta-i}}{(\varepsilon - \varepsilon_{k\beta})^2 - 4t^2} f_\beta(\varepsilon_{k\beta}) \tag{7}$$

$$\tilde{\Sigma}_{i-i}(\varepsilon) = -\sum_{k,\beta} \frac{T^*_{k\beta i}T_{k\beta-i}}{\varepsilon - \varepsilon_{k\beta}} f_\beta(\varepsilon_{k\beta}) + \sum_{k,\beta} \frac{t\left(\left|T_{k\beta i}\right|^2 + \left|T_{k\beta-i}\right|^2\right)}{(\varepsilon - \varepsilon_{k\beta})^2 - 4t^2} f_\beta(\varepsilon_{k\beta}) - \sum_{k,\beta} \frac{4t^2T^*_{k\beta i}T_{k\beta-i}}{(\varepsilon - \varepsilon_{k\beta})[(\varepsilon - \varepsilon_{k\beta})^2 - 4t^2]} f_\beta(\varepsilon_{k\beta}). \tag{8}$$

Advanced $\hat{G}^{\mathrm{a}}$ and retarded $\hat{G}^{\mathrm{r}} = (\hat{G}^{\mathrm{a}})^\dagger$ functions are found with the use of Dyson equation (5), whereas the lesser one $\hat{G}^<$ is determined from the Keldysh formula $\hat{G}^< = \hat{G}^{\mathrm{r}}\hat{\Sigma}^<\hat{G}^{\mathrm{a}}$ with the self-energy $\hat{\Sigma}^<$ calculated applying the Ng ansatz [17]: $\hat{\Sigma}^< = \hat{\Sigma}^<_0\hat{\Gamma}^{-1}\hat{\Gamma}^{\mathrm{ef}}$ where $\hat{\Sigma}^<_0 = \mathrm{i}(\hat{\Gamma}^{\mathrm{L}}f_{\mathrm{L}} + \hat{\Gamma}^{\mathrm{R}}f_{\mathrm{R}})$, $\hat{\Gamma} = \hat{\Gamma}^{\mathrm{L}} + \hat{\Gamma}^{\mathrm{R}} = \mathrm{i}(\hat{\Sigma}^{\mathrm{r}}_0 - \hat{\Sigma}^{\mathrm{a}}_0)$ and $\hat{\Gamma}^{\mathrm{ef}} = \mathrm{i}(\hat{\Sigma}^{\mathrm{r}} - \hat{\Sigma}^{\mathrm{a}})$. The knowledge of $G^<$ allows one to determine the electric current flowing through the system (equation (4)) as well as mean values $\langle d^+_i d_{i'}\rangle = -\mathrm{i}\int \frac{\mathrm{d}\varepsilon}{2\pi} G^<_{i'i}$ which are calculated self-consistently. The linear conductance G in the limit of a weak bias voltage (at equilibrium) is given by $G = \frac{2\mathrm{e}^2}{h}\int \mathrm{d}\varepsilon T(\varepsilon)(-\frac{\partial f}{\partial \varepsilon})$, where the total transmission is equal to $T(\varepsilon) = \frac{1}{2}\mathrm{Tr}[\hat{\Gamma}^{\mathrm{L}}\hat{G}^{\mathrm{r}}\hat{\tilde{\Gamma}}^{\mathrm{R}}\hat{G}^{\mathrm{a}} + \hat{\Gamma}^{\mathrm{R}}\hat{G}^{\mathrm{r}}\hat{\tilde{\Gamma}}^{\mathrm{L}}\hat{G}^{\mathrm{a}}]$ with $\hat{\tilde{\Gamma}}^{\beta} = \hat{\Gamma}^{\beta}\hat{\Gamma}^{-1}\hat{\Gamma}^{\mathrm{eff}}$ (for more details see [12]).

3. Results and discussion

For simplicity we assume that energy levels of both dots are aligned with $E_1 = E_2 = E_0$. To take into account mixing effects between two channels the parameter α is introduced which changes from 0, with no cross-coupling effects included, to 1, which corresponds to maximal mixing when two QDs are coupled to common left and right reservoirs. As the situation for $\alpha \neq 0$ is to some extent analogous to systems with ferromagnetic electrodes of non-collinear magnetizations where during tunnelling processes the electron spin rotates about a definite angle ϑ [32, 46, 48] it is reasonable to express diagonal and non-diagonal tunnelling rates in the following form: $\Gamma^\beta_{ii} = \Gamma^\beta/(1+\alpha)$ and $\Gamma^\beta_{i-i} = \Gamma^\beta\alpha/(1+\alpha)$. Couplings to the leads are then normalized and they are proportional to $\cos^2\vartheta = 1/(1+\alpha)$ and $\sin^2\vartheta = \alpha/(1+\alpha)$, respectively. Γ, which represents here the dot–lead coupling strength, is taken as the energy unit. Calculations are performed for strongly correlated systems in the limit of infinite U. The band width in electrodes is assumed to be equal to 500Γ.

The density of states (DOS) calculated for $\alpha = 0$ is plotted in figure 2. As both dots are identical the spectral density is presented for one dot only. In the absence of cross-coupling effects ($\alpha = 0$) the orbital pseudo-spin is conserved during tunnelling processes and for $t = 0$ two dots are capacitively coupled. Accordingly, a well-defined peak pinned to the Fermi level of the leads ($E_{\mathrm{F}} = 0$ for $eV = 0$) can be observed. The intensity, as well as the width of the peak, strongly depends on the temperature (figure 2(a)), so the peak shows features typical of the Kondo anomaly. When the coupling between dots is introduced the Kondo peak splits into two components centred at $\varepsilon = \pm 2t$. In this case electron transport takes place through two molecular states split by $2t$. After applying a bias voltage to the system an additional splitting

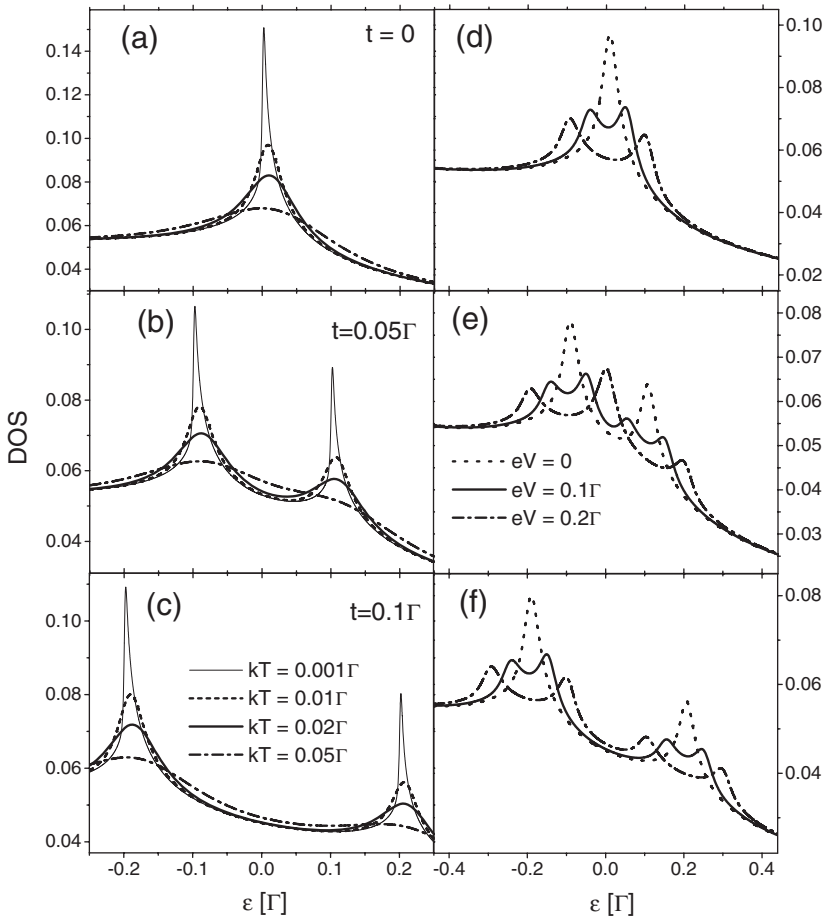

Figure 2. Local densities of states in the Kondo regime ($E_0 = -4\Gamma$) for $\alpha = 0$ and indicated values of temperature kT (left panel, $eV = 0$) and bias voltage eV (right panel, $kT = 0.01\Gamma$), $\Gamma^{\mathrm{L}} = \Gamma^{\mathrm{R}} = \Gamma$.

of each Kondo anomaly appears and the components are pinned at Fermi levels of the left and right electrodes which differ by eV (figures 2(d)–(f)).

The differential conductance $G_{\mathrm{diff}} = \mathrm{d}I/\mathrm{d}V$ calculated for $\alpha = 0$ and several values of inter-dot tunnelling rate t is depicted in figure 3. For the system with symmetric couplings to electrodes $\Gamma^{\mathrm{L}} = \Gamma^{\mathrm{R}} = \Gamma$ and energy levels of both dots aligned the results are fully symmetric with respect to the bias reversal as presented in figure 3(a). When dots are capacitively coupled ($t = 0$) a pronounced peak appears in a zero bias regime, which is good evidence for the Kondo anomaly in the system. Inter-dot tunnelling effects lead to strong modifications of the conductance curves. With increase of t the Kondo peak at first decreases and then splits into two components centred at $eV = \pm 2t$. The intensities of the components decrease strongly for higher values of t. The behaviour of the orbital Kondo anomaly obtained here is very similar to the one typical of the spin Kondo phenomenon in the presence of an external field [39, 40]. The result is also qualitatively consistent with experimental data [38]. When coupling strengths to both electrodes are considerably different ($\Gamma^{\mathrm{L}} \neq \Gamma^{\mathrm{R}}$) the intensity of the peak corresponding to $t = 0$ is strongly reduced in comparison to the symmetrical case (figure 3(b)). As

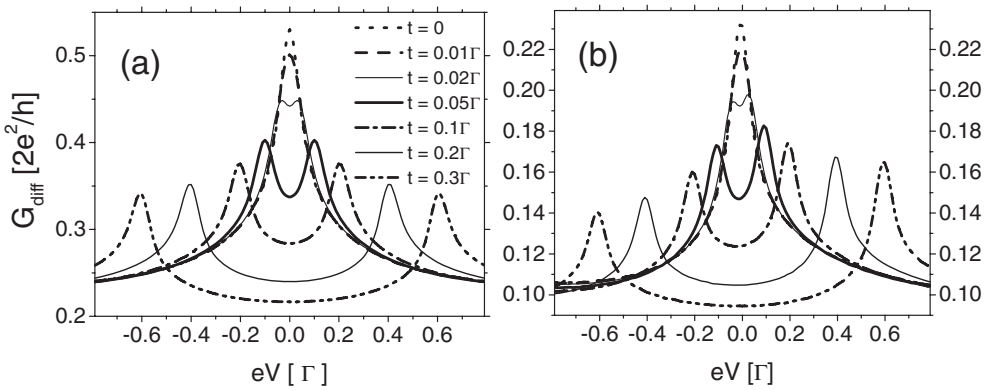

Figure 3. Bias dependence of differential conductance for indicated values of t. The relevant parameters are as follows: $E_0 = -4\Gamma, \alpha = 0$ and $kT = 0.01\Gamma$; (a) symmetric case with $\Gamma^{\mathrm{L}} = \Gamma^{\mathrm{R}} = \Gamma$, (b) $\Gamma^{\mathrm{L}}_{11} = \Gamma^{\mathrm{L}}_{22} = 1.75\Gamma$ and $\Gamma^{\mathrm{R}}_{11} = \Gamma^{\mathrm{R}}_{22} = 0.25\Gamma$.

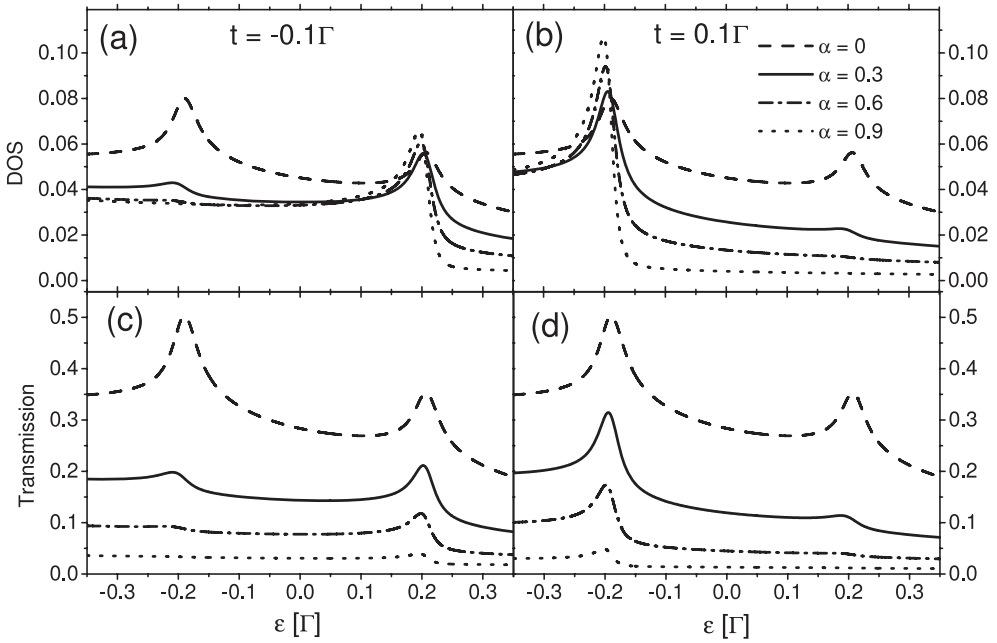

Figure 4. Density of states and transmission for different cross-coupling parameters α and $kT = 0.01\Gamma$, $E_0 = -4\Gamma$, $\Gamma^{\mathrm{L}} = \Gamma^{\mathrm{R}} = \Gamma$, (left panel: $t = -0.1\Gamma$ and right panel: $t = 0.1\Gamma$).

inter-dot coupling is introduced, the anomaly becomes split and the intensities of both components are additionally lowered. Moreover, the conductance curves reveal some asymmetry which is more pronounced for higher coupling rates. It can be mentioned that similar asymmetry in the differential conductance was observed experimentally, but for a double occupied carbon nanotube QD [41].

Consider now the channel mixing effects and their influence on the Kondo phenomenon. The spectral density (DOS) and the transmission $T(\varepsilon)$ are depicted in figure 4 for two values of tunnelling rate t and different cross-coupling parameters α. When $\alpha = 0$ the DOS exhibits

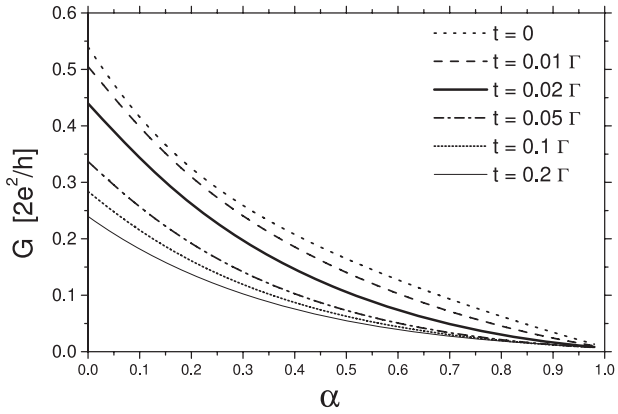

Figure 5. The linear conductance as a function of cross-coupling parameter α for indicated values of inter-dot coupling t. The other parameters are $kT = 0.01\Gamma$, $E_0 = -4\Gamma$, $\Gamma^{\mathrm{L}} = \Gamma^{\mathrm{R}} = \Gamma$.

two well-defined Kondo peaks centred at $\varepsilon = \pm 2t$ and the curves are identical for $t = 0.1\Gamma$ and -0.1Γ. With mixing effects included they start to differ considerably. The intensity of the peak centred at $\varepsilon = -2t$ (for positive and negative values of t) increases with increase of α and the peak becomes strongly asymmetric. Just after the peak the DOS sharply decreases and at higher values of α it is considerably suppressed. At the same time the intensity of the second component corresponding to $\varepsilon = 2t$ decreases and finally the resonance disappears. Due to these modifications the spectral functions corresponding to attractive ($t < 0$) and repulsive ($t > 0$) inter-dot coupling differ considerably.

Mixing effects strongly influence the transmission function $T(\varepsilon)$, which is also displayed in figure 4 ((c) and (d)). As the conservation of pseudo-spin is broken, transmission is suppressed for higher values of α. The intensity of both Kondo components present in $T(\varepsilon)$ decreases and they disappear as α approaches 1 with maximal mixing of both channels. In such a situation tunnelling electrons lose information about their pseudo-spin orientation, and the orbital Kondo effect vanishes.

The tendency to suppress the Kondo anomaly due to channel mixing as well as due to inter-dot coupling can be also seen in the linear and differential conductance. The linear spectra in the Kondo regime as functions of the mixing parameter α are presented in figure 5 for several values of t. The conductance decreases monotonically as α changes from 0 to 1, and cross-coupling effects become important. Suppression of the conductance is much more pronounced when inter-dot tunnelling processes are included. In such a case the splitting additionally destroys the Kondo effect. A similar conclusion can be drawn by analysing the differential conductance. The appropriate curves calculated in the Kondo regime for several values of hopping rate t and different values of α are presented in figure 6. The zero-bias maximum can be easily seen for the case of uncoupled dots ($t = 0$). The intensity of the Kondo peak gradually decreases as mixing effects are included and the anomaly is suppressed in the presence of strong channel mixing ($\alpha \approx 1$). For $t \neq 0$, splitting of the main peak originating from the inter-dot coupling is obtained. The intensities of these components decrease strongly as mixing effects become important. For high values of α the calculated curves are flat with only some remnants of the Kondo anomaly.

Next, the linear conductance as a function of a dot level position E_0 tuned by a gate voltage is investigated. Spectra calculated for various values of α are plotted in figure 7. For $\alpha = 0$ and a small inter-dot coupling ($t = 0.02\Gamma$) the main peak appears in the Kondo regime. It should

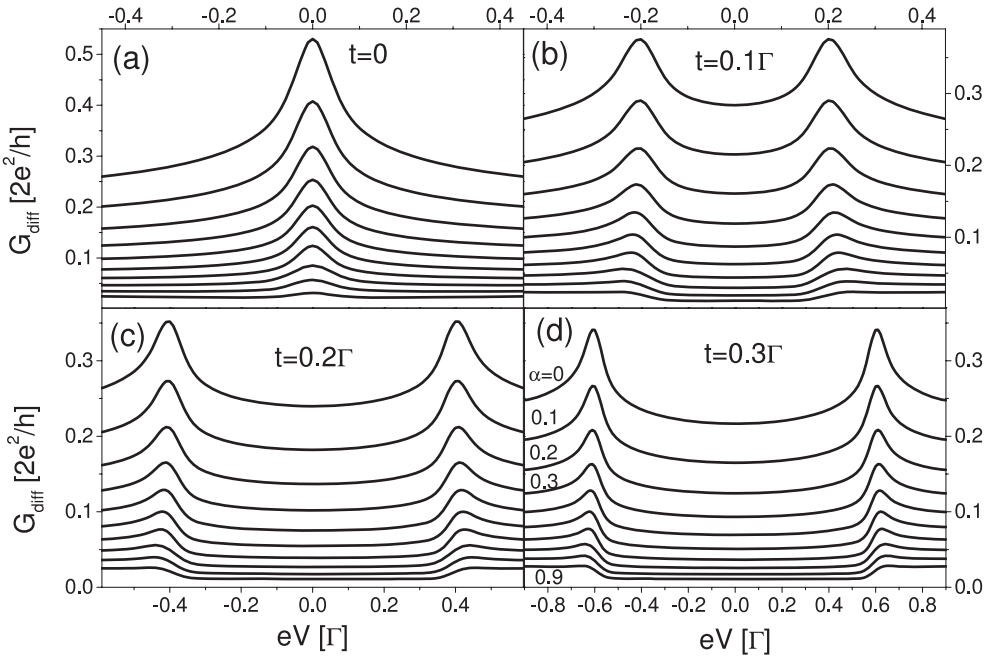

Figure 6. Bias dependence of differential conductance for different values of hopping rate t and cross-coupling parameter α, $kT = 0.01\Gamma$, $E_0 = -4\Gamma$, $\Gamma^{\mathrm{L}} = \Gamma^{\mathrm{R}} = \Gamma$.

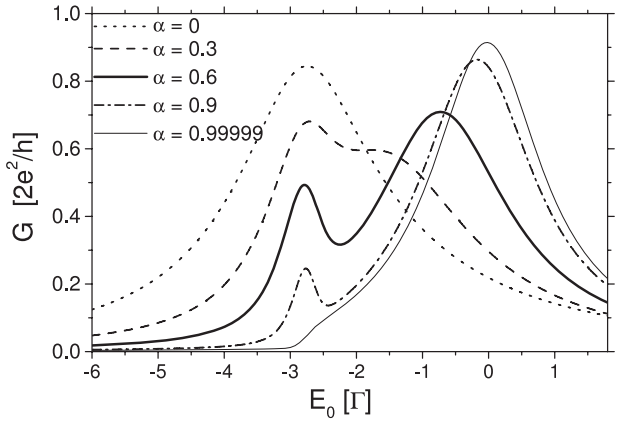

Figure 7. The linear conductance as a function of dot level position E_0 for indicated values of α, $t = 0.02\Gamma$ and $kT = 0.01\Gamma$, $\Gamma^{\mathrm{L}} = \Gamma^{\mathrm{R}} = \Gamma$.

be pointed out that the present approach corresponds to relatively high temperatures, namely close to the Kondo one. It is a consequence of the decoupling procedure of higher-order GFs used in the EOM [49, 51]. Accordingly, the unitary limit or a wide plateau, which are typical features of the zero-temperature Kondo phenomenon, cannot be achieved within the framework of the approach. However, the obtained results constitute a good qualitative picture appropriate for non-zero temperatures [50].

The results presented in figure 7 well confirm the conclusion that channel mixing effects destroy the Kondo anomaly and lead to the suppression of the conductance in the Kondo

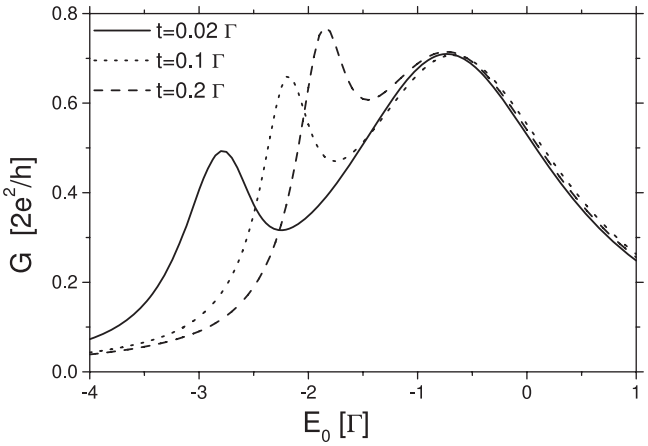

Figure 8. The linear conductance as a function of dot level position E_0 for indicated values of coupling between two dots t. The other parameters are $\alpha = 0.6, kT = 0.01\Gamma$ and $\Gamma^{\mathrm{L}} = \Gamma^{\mathrm{R}} = \Gamma$.

regime. However, at intermediate values of α and non-vanishing coupling between two dots ($t \neq 0$) interference effects take place which lead to a relatively small but well-pronounced side peak. This side-band maximum disappears as α approaches 1 with two dots attached to common reservoirs, which corresponds to the parallel configuration. For intermediate values of α the intensity, as well as the position of the side peak, strongly depends on the inter-dot tunnelling rate, which is well illustrated in figure 8. With increase of t the side peak is much more pronounced and it is shifted towards energies closer to the Fermi level. At the same time the position of the main wide maximum remains practically unchanged.

Analysis of the spectral density curves calculated for dot level in the Kondo regime as well as for E_0 corresponding to side maxima in G appearing at different values of the coupling rate t allows one to understand the results (figure 9). In the Kondo regime sharp peaks centred at $\varepsilon = -2t$ can be seen, but the DOS due to level splitting and channel mixing effects is strongly suppressed near the Fermi energy E_{F} (figure 9(a)), and therefore the current is blocked in a low-bias regime. When the dot level E_0 is shifted towards higher energies the appropriate peak is also moved and it crosses the Fermi level leading to the side maximum in the conductance spectrum. For greater t the crossing takes place at higher energy, E_0. All these effects explain the behaviour of the conductance presented in figure 8 well.

The differential conductance calculated for E_0 corresponding to the side maximum for $t = 0.1\Gamma$ and $\alpha = 0.6$ is displayed in figure 10. One can see that a round but well-pronounced zero-bias peak is obtained instead of two low-intensity components present in G_{diff} corresponding to the Kondo regime (see figure 6(b)).

4. Summary and conclusions

We have studied electron transport through the parallel DQD system and analysed the influence of channel mixing effects on the orbital Kondo phenomenon. In consistency with other theoretical approaches [32, 33] we find that cross-couplings present in the system strongly influence the effect, leading to a suppression of the Kondo resonance. The present work provides a detailed analysis of the effect in the linear and nonlinear transport regimes, whereas the previous ones were mainly limited to equilibrium situation. If dots are capacitively coupled ($t = 0$) a zero-bias well-pronounced Kondo peak can be observed in the differential

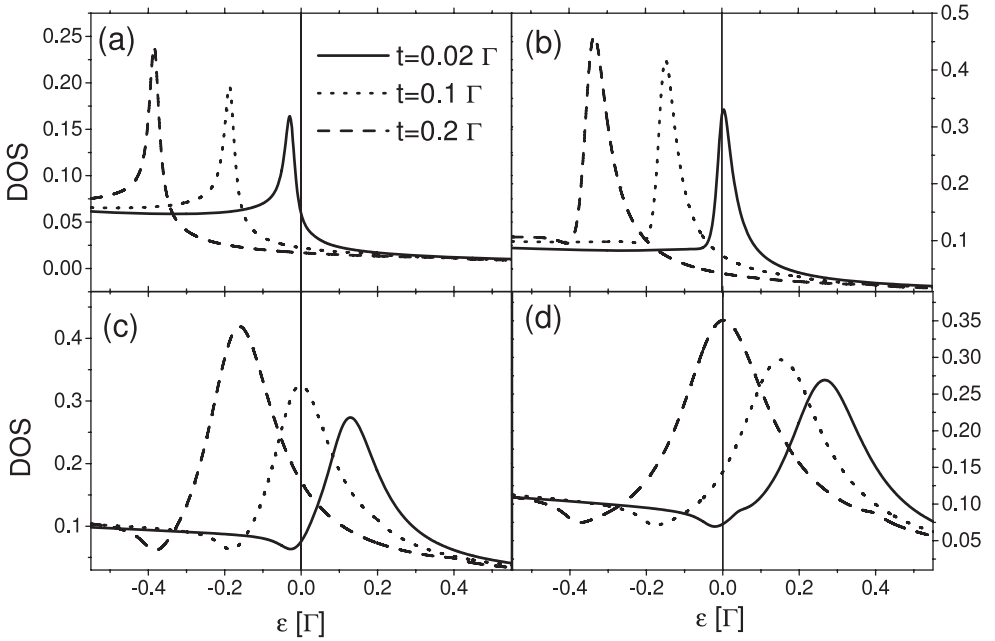

Figure 9. Density of states for indicated values of t and $\alpha = 0.6$, $kT = 0.01\Gamma$, $\Gamma^{\mathrm{L}} = \Gamma^{\mathrm{R}} = \Gamma$. The curves are calculated for a dot level in the Kondo regime (a: $E_0 = -4\Gamma$) as well as for E_0 corresponding to side maxima in G appearing at different values of coupling rate t (b: $E_0 = -2.8\Gamma$), (c: $E_0 = -2.2\Gamma$), (d: $E_0 = -1.9\Gamma$).

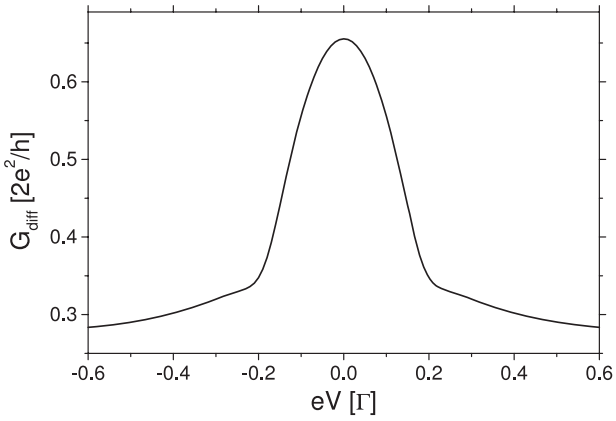

Figure 10. Bias dependence of differential conductance for $E_0 = -2.2\Gamma$, $t = 0.1\Gamma$, $\alpha = 0.6$, $kT = 0.01\Gamma$ and $\Gamma^{\mathrm{L}} = \Gamma^{\mathrm{R}} = \Gamma$.

conductance for $\alpha = 0$ (no mixing present). With increase of α the peak intensity gradually diminishes, and finally, the resonance disappears when α is equal to 1. For high values of α the linear conductance is considerably suppressed in the Kondo regime. Direct tunnel coupling between dots also leads to a suppression of the Kondo anomaly due to a splitting of the resonance peak. The result is consistent with experimental data and theoretical analysis performed by Holleitner *et al* [38]. Moreover, the present studies reveal that in a DQD system with inter-dot coupling and channel mixing effects taken into account interference processes

can influence the conductance spectra, leading to a well-pronounced side peak. The intensity of the peak increases with the coupling rate t. At the same time its position shifts towards higher energies, whereas a strong suppression of the conductance in the Kondo regime can be observed.

Appendix

We present here details of calculations based on the equation of motion method which allow one to obtain the Dyson equation for the GF used in section 2. Writing equations of motion for $G_{11}(\varepsilon) = \langle\langle d_1, d_1^+\rangle\rangle$ and $G_{21}(\varepsilon) = \langle\langle d_2, d_1^+\rangle\rangle$, one finds

$$(\varepsilon - E_1 - \Sigma_{011})G_{11} = 1 + U\langle\langle d_1 d_2^+ d_2, d_1^+\rangle\rangle + (t + \Sigma_{012})G_{21} \tag{A.1a}$$

$$(\varepsilon - E_2 - \Sigma_{022})G_{21} = U\langle\langle d_2 d_1^+ d_1, d_1^+\rangle\rangle + (t + \Sigma_{021})G_{11} \tag{A.1b}$$

where the term $\Sigma_{0ij} = \sum_{k\beta} T^*_{k\beta i} T_{k\beta j}/(\varepsilon - \varepsilon_{k\beta})$ describes the self-energy of a non-interacting system. Applying the EOM to the two new GFs that appear on the right-hand side of equations (A.1*a*) and (A.1*b*), one gets

$$\begin{aligned}(\varepsilon - E_1 - U)\langle\langle d_1 d_2^+ d_2, d_1^+\rangle\rangle &= n_2 + t\langle\langle d_2 d_1^+ d_1, d_1^+\rangle\rangle + \sum_{k,\beta}\big\{T^*_{k\beta 1}\langle\langle a_{k\beta} d_2^+ d_2, d_1^+\rangle\rangle \\ &\quad - T^*_{k\beta 2}\langle\langle a_{k\beta} d_2^+ d_1, d_1^+\rangle\rangle + T_{k\beta 2}\langle\langle a_{k\beta}^+ d_1 d_2, d_1^+\rangle\rangle\big\}\end{aligned} \tag{A.2a}$$

$$\begin{aligned}(\varepsilon - E_2 - U)\langle\langle d_2 d_1^+ d_1, d_1^+\rangle\rangle &= -\langle d_1^+ d_2\rangle + t\langle\langle d_1 d_2^+ d_2, d_1^+\rangle\rangle + \sum_{k,\beta}\big\{T^*_{k\beta 2}\langle\langle a_{k\beta} d_1^+ d_1, d_1^+\rangle\rangle \\ &\quad - T^*_{k\beta 1}\langle\langle a_{k\beta} d_1^+ d_2, d_1^+\rangle\rangle + T_{k\beta 1}\langle\langle a_{k\beta}^+ d_2 d_1, d_1^+\rangle\rangle\big\}\end{aligned} \tag{A.2b}$$

where $n_i = \langle d_i^+ d_i\rangle$ describes the mean number of electrons in the dot $i = 1, 2$. In the above equations new GFs $\langle\langle a_{k\beta} d_2^+ d_2, d_1^+\rangle\rangle$, $\langle\langle a_{k\beta} d_2^+ d_1, d_1^+\rangle\rangle$, $\langle\langle a_{k\beta}^+ d_1 d_2, d_1^+\rangle\rangle$, $\langle\langle a_{k\beta} d_1^+ d_1, d_1^+\rangle\rangle$, $\langle\langle a_{k\beta} d_1^+ d_2, d_1^+\rangle\rangle$ appear. For example the EOM for $\langle\langle a_{k\beta} d_2^+ d_1, d_1^+\rangle\rangle$ is written as

$$\begin{aligned}(\varepsilon - \varepsilon_{k\beta} - E_1 + E_2)\langle\langle a_{k\beta} d_2^+ d_1, d_1^+\rangle &= -\langle d_2^+ a_{k\beta}\rangle + t\langle\langle a_{k\beta} d_2^+ d_2, d_1^+\rangle\rangle \\ &\quad - t\langle\langle a_{k\beta} d_1^+ d_1, d_1^+\rangle\rangle - T_{k\beta 2}\langle\langle d_1 d_2^+ d_2, d_1^+\rangle\rangle + \sum_p T_{p\beta 2}\langle\langle a_{p\beta}^+ a_{k\beta} d_1, d_1^+\rangle\rangle.\end{aligned} \tag{A.3}$$

Now, the decoupling scheme proposed by Meir [49] is applied to the higher-order GFs. According to the procedure, functions which contain two lead operators are decoupled as follows:

$$\langle\langle a_{p\beta}^+ a_{k\beta} d_1, d_1^+\rangle\rangle = \langle a_{p\beta}^+ a_{k\beta}\rangle\langle\langle d_1, d_1^+\rangle\rangle = \delta_{pk} f_\beta(\varepsilon_{k\beta})\langle\langle d_1, d_1^+\rangle\rangle \tag{A.4}$$

whereas mean values of the type $\langle d_i^+ a_{k\beta}\rangle$ are neglected [51]. Then, equation (A.3) takes the form

$$\begin{aligned}(\varepsilon - \varepsilon_{k\beta} - E_1 + E_2)\langle\langle a_{k\beta} d_2^+ d_1, d_1^+\rangle\rangle &= t\langle\langle a_{k\beta} d_2^+ d_2, d_1^+\rangle\rangle - t\langle\langle a_{k\beta} d_1^+ d_1, d_1^+\rangle\rangle \\ &\quad - T_{k\beta 2}\langle\langle d_1 d_2^+ d_2, d_1^+\rangle\rangle + T_{k\beta 2} f_\beta(\varepsilon_{k\beta})\langle\langle d_1, d_1^+\rangle\rangle.\end{aligned} \tag{A.5}$$

It is worth mentioning that no approximation or decoupling is made for the higher-order GFs that correspond only to the dots. Writing equations for other GFs which contain only one lead operator and applying the similar decoupling procedure, one finds

$$\begin{aligned}(\varepsilon - \varepsilon_{k\beta})\langle\langle a_{k\beta} d_2^+ d_2, d_1^+\rangle\rangle &= t\langle\langle a_{k\beta} d_2^+ d_1, d_1^+\rangle\rangle - t\langle\langle a_{k\beta} d_1^+ d_2, d_1^+\rangle\rangle + T_{k\beta 1}\langle\langle d_1 d_2^+ d_2, d_1^+\rangle\rangle \\ &\quad + T_{k\beta 2} f_\beta(\varepsilon_{k\beta})\langle\langle d_2, d_1^+\rangle\rangle\end{aligned} \tag{A.6}$$

$$\begin{aligned}(\varepsilon - \varepsilon_{k\beta} + E_1 - E_2)\langle\langle a_{k\beta} d_1^+ d_2, d_1^+\rangle\rangle &= t\langle\langle a_{k\beta} d_1^+ d_1, d_1^+\rangle\rangle - t\langle\langle a_{k\beta} d_2^+ d_2, d_1^+\rangle\rangle \\ &\quad - T_{k\beta 1}\langle\langle d_2 d_1^+ d_1, d_1^+\rangle\rangle + T_{k\beta 1} f_\beta(\varepsilon_{k\beta})\langle\langle d_2, d_1^+\rangle\rangle\end{aligned} \tag{A.7}$$

$$(\varepsilon - \varepsilon_{k\beta})\langle\langle a_{k\beta}d_1^+d_1, d_1^+\rangle\rangle = t\langle\langle a_{k\beta}d_1^+d_2, d_1^+\rangle\rangle - t\langle\langle a_{k\beta}d_2^+d_1, d_1^+\rangle\rangle + T_{k\beta 2}\langle\langle d_2d_1^+d_1, d_1^+\rangle\rangle + T_{k\beta 1}f_\beta(\varepsilon_{k\beta})\langle\langle d_1, d_1^+\rangle\rangle \quad (A.8)$$

$$(\varepsilon + \varepsilon_{k\beta} - E_1 - E_2 - U)\langle\langle a_{k\beta}^+d_1d_2, d_1^+\rangle\rangle = -T_{k\beta 1}^*\langle\langle d_2d_1^+d_1, d_1^+\rangle\rangle + T_{k\beta 1}^*f_\beta(\varepsilon_{k\beta})\langle\langle d_2, d_1^+\rangle\rangle - T_{k\beta 2}^*f_\beta(\varepsilon_{k\beta})\langle\langle d_1, d_1^+\rangle\rangle + T_{k\beta 2}^*\langle\langle d_1d_2^+d_2, d_1^+\rangle\rangle. \quad (A.9)$$

A closed set of equations (A.5)– (A.9) is then obtained which can be easily solved. Next the solutions are substituted into equation (A2), which leads to a set of two linear equations:

$$A\langle\langle d_1d_2^+d_2, d_1^+\rangle\rangle - \tilde{t}\langle\langle d_2d_1^+d_1, d_1^+\rangle\rangle = \langle n_2\rangle - \Sigma_2^M\langle\langle d_1, d_1^+\rangle\rangle - \Sigma^P\langle\langle d_2, d_1^+\rangle\rangle \quad (A.10)$$

$$-\tilde{t}\langle\langle d_1d_2^+d_2, d_1^+\rangle\rangle + B\langle\langle d_2d_1^+d_1, d_1^+\rangle\rangle = -\langle d_1^+d_2\rangle - \Sigma_1^M\langle\langle d_2, d_1^+\rangle\rangle - \Sigma^P\langle\langle d_1, d_1^+\rangle\rangle \quad (A.11)$$

which allow one to express the second-order functions $\langle\langle d_1d_2^+d_2, d_1^+\rangle\rangle$, $\langle\langle d_2d_1^+d_1, d_1^+\rangle\rangle$ in terms of $\langle\langle d_1, d_1^+\rangle\rangle$ and $\langle\langle d_2, d_1^+\rangle\rangle$. To simplify the notation, we define

$$A = \varepsilon - E_1 - U - \Sigma_{011} - \Sigma_{11}^{c(0)} - \Sigma_{22}^{e(0)} - \Sigma_{22}^{d(0)} + \Sigma_{12}^{a(0)} + \Sigma_{21}^{a(0)}$$

$$B = \varepsilon - E_2 - U - \Sigma_{022} - \Sigma_{22}^{c(0)} - \Sigma_{11}^{f(0)} - \Sigma_{11}^{d(0)} + \Sigma_{12}^{b(0)} + \Sigma_{21}^{b(0)}$$

$$\tilde{t} = t + \Sigma_{22}^{a(0)} + \Sigma_{11}^{b(0)} - \Sigma_{12}^{c(0)} - \Sigma_{21}^{c(0)} - \Sigma_{21}^{d(0)}$$

$$\Sigma_1^M = \Sigma_{22}^{c(1)} + \Sigma_{11}^{f(1)} + \Sigma_{11}^{d(1)} - \Sigma_{12}^{b(1)} - \Sigma_{21}^{b(1)}$$

$$\Sigma_2^M = \Sigma_{11}^{c(1)} + \Sigma_{22}^{e(1)} + \Sigma_{22}^{d(1)} - \Sigma_{12}^{a(1)} - \Sigma_{21}^{a(1)}$$

$$\Sigma^P = \Sigma_{22}^{a(1)} + \Sigma_{11}^{b(1)} - \Sigma_{21}^{d(1)} - \Sigma_{21}^{g(1)} - \Sigma_{12}^{c(1)} - \Sigma_{21}^{c(1)}$$

where the self-energies are defined as

$$\Sigma_{ij}^{a(n)} = \sum_{k,\beta} T_{k\beta i}^* T_{k\beta j} \frac{t(\varepsilon - \varepsilon_{k\beta} + E_1 - E_2)}{d} F_\beta^{(n)}(\varepsilon_{k\beta})$$

$$\Sigma_{ij}^{b(n)} = \sum_{k,\beta} T_{k\beta i}^* T_{k\beta j} \frac{t(\varepsilon - \varepsilon_{k\beta} - E_1 + E_2)}{d} F_\beta^{(n)}(\varepsilon_{k\beta})$$

$$\Sigma_{ij}^{c(n)} = \sum_{k,\beta} T_{k\beta i}^* T_{k\beta j} \frac{2t^2}{\mathrm{d}} F_\beta^{(n)}(\varepsilon_{k\beta})$$

$$\Sigma_{ij}^{d(n)} = \sum_{k,\beta} \frac{T_{k\beta i}^* T_{k\beta j}}{\varepsilon + \varepsilon_{k\beta} - E_1 - E_2 - U} F_\beta^{(n)}(\varepsilon_{k\beta})$$

$$\Sigma_{ij}^{e(n)} = \sum_{k,\beta} T_{k\beta i}^* T_{k\beta j} \frac{(\varepsilon - \varepsilon_{k\beta})(\varepsilon - \varepsilon_{k\beta} + E_1 - E_2) - 2t^2}{d} F_\beta^{(n)}(\varepsilon_{k\beta})$$

$$\Sigma_{ij}^{f(n)} = \sum_{k,\beta} T_{k\beta i}^* T_{k\beta j} \frac{(\varepsilon - \varepsilon_{k\beta})(\varepsilon - \varepsilon_{k\beta} - E_1 + E_2) - 2t^2}{d} F_\beta^{(n)}(\varepsilon_{k\beta})$$

$$\Sigma_{ij}^{g(1)} = \sum_{k,\beta} \frac{T_{k\beta i}^* T_{k\beta j}}{\varepsilon - \varepsilon_{k\beta}} f_\beta(\varepsilon_{k\beta})$$

with $d = (\varepsilon - \varepsilon_{k\beta})[(\varepsilon - \varepsilon_{k\beta} + E_1 - E_2)(\varepsilon - \varepsilon_{k\beta} - E_1 + E_2) - 4t^2]$, $F_\beta^{(1)}(\varepsilon_{k\beta}) = f_\beta(\varepsilon_{k\beta})$ and $F_\beta^{(0)}(\varepsilon_{k\beta}) = 1$.

Finally, GFs $G_{ij} = \langle\langle d_i, d_j^+\rangle\rangle$ are calculated in the limit of infinite U and they are written in the matrix form which corresponds to the Dyson equation (equation (5) in the text): $\hat{G}(\varepsilon) = [\hat{I} - \hat{g}(\varepsilon)\hat{\Sigma}(\varepsilon)]^{-1}\hat{g}(\varepsilon)$, where $\hat{g}(\varepsilon)$ is the GF of the DQD region in the absence of any coupling or interaction and $\hat{\Sigma}$ describes the appropriate self-energy. Explicit forms of these matrices are given in the text for equal level positions $E_1 = E_2 = E_0$.

References

[1] DiVincenzo D P 1995 *Phys. Rev.* A **51** 1015
[2] Loss D and DiVincenzo D P 1998 *Phys. Rev.* A **57** 120
Loss D and Sukhorukov E V 2000 *Phys. Rev. Lett.* **84** 1035
[3] Goldhaber-Gordon D, Shtrikman H, Mahalu D, Abusch-Magder D, Meirav U and Kastner M A 1998 *Nature* **391** 156
[4] Gores J, Goldhaber-Gordon D, Heemeyer S, Kastner M A, Shtrikman H, Mahalu D and Meirav U 2000 *Phys. Rev.* B **62** 2188
[5] Sasaki S, De Franceschi S, Elzerman J M, van der Wiel W G, Eto M, Tarucha S and Kouwenhoven L P 2000 *Nature* **405** 764
[6] van der Wiel W G, De Franceschi S, Fujisawa T, Elzerman J M, Tarucha S and Kouwenhoven L P 2000 *Science* **289** 2105
[7] Johnson A C, Marcus C M, Hanson M P and Gossard A C 2004 *Phys. Rev. Lett.* **93** 106803
[8] Kobayashi K, Aikawa H, Katsumoto S and Iye Y 2002 *Phys. Rev. Lett.* **88** 256806
Kobayashi K, Aikawa H, Katsumoto S and Iye Y 2003 *Phys. Rev.* B **68** 235304
[9] Holleitner A W, Decker C R, Qin H, Eberl K and Blick R H 2001 *Phys. Rev. Lett.* **87** 256802
[10] Zacharia I G, Goldhaber-Gordon D, Granger G, Kastner M A and Khavin Yu B 2001 *Phys. Rev.* B **64** 155311
[11] Ladron de Guevara M L, Claro F and Orellana P A 2003 *Phys. Rev.* B **67** 195335
Orellana P A, Ladron de Guevara M L and Claro F 2004 *Phys. Rev.* B **70** 233315
[12] Sztenkiel D and Swirkowicz R 2007 *J. Phys.: Condens. Matter* **19** 176202
[13] Tanaka Y and Kawakami N 2005 *Phys. Rev.* B **72** 085304
[14] Rushforth A W, Smith C G, Farrer I, Ritchie D A, Jones G A, Anderson D and Pepper M 2006 *Phys. Rev.* B **73** 081305
[15] Stefański P, Tagliacozzo A and Bułka B R 2004 *Phys. Rev. Lett.* **93** 186805
Bułka B R and Stefański P 2001 *Phys. Rev. Lett.* **86** 5128
[16] Ding G-H, Kim C K and Nahm K 2005 *Phys. Rev.* B **71** 205313
[17] Ng T K and Lee P A 1988 *Phys. Rev. Lett.* **61** 1768
[18] Jeong H, Chang A M and Melloch M R 2001 *Science* **293** 2221
[19] Aono T and Eto M 2001 *Phys. Rev.* B **63** 125327
[20] Aguado R and Langreth D C 2003 *Phys. Rev.* B **67** 245307
[21] Ivanov T 1997 *Europhys. Lett.* **40** 183
[22] Georges A and Meir Y 1999 *Phys. Rev. Lett.* **82** 3508
[23] Sakano R and Kawakami N 2006 *Phys. Rev.* B **73** 155332
Grobis M, Rau I G, Potok R M and Goldhaber-Gordon D 2006 *Preprint* cond-mat/0611480
[24] Jarillo-Herrero P, Kong J, van der Zant H S J, Dekker C, Kouwenhoven L P and De Franceschi S 2005 *Phys. Rev. Lett.* **94** 156802
[25] Sasaki S, Amaha S, Asakawa N, Eto M and Tarucha S 2004 *Phys. Rev. Lett.* **93** 017205
Tokura Y, Sasaki S, Austing D G and Tarucha S 2001 *Physica* B **298** 260
[26] Sato T and Eto M 2005 *Physica* E **29** 652
[27] Le Hur K, Simon P and Borda L 2004 *Phys. Rev.* B **69** 045326
Le Hur K, Simon P and Loss D 2007 *Phys. Rev.* B **75** 035332
[28] López R, Sánchez D, Lee M, Choi M-S, Simon P and Le Hur K 2005 *Phys. Rev.* B **71** 115312
[29] Galpin M R, Logan D E and Krishnamurthy H R 2005 *Phys. Rev. Lett.* **94** 186406
[30] Zarand G, Brataas A and Goldhaber-Gordon D 2003 *Solid State Commun.* **126** 463
[31] Borda L, Zarand G, Hofstetter W, Halperin B I and von Delft J 2003 *Phys. Rev. Lett.* **90** 026602
[32] Lim J S, Choi M-S, Choi M Y, López R and Aguado R 2006 *Phys. Rev.* B **74** 205119
[33] Chudnovskiy A L 2006 *Physica* E **34** 385
[34] Choi M-S, Lopez R and Aguado R 2005 *Phys. Rev. Lett.* **95** 067204
[35] Pohjola T, Boese D, Schoeller H, Konig J and Schon G 2000 *Physica* B **284–288** 1762
Pohjola T, Boese D, Konig J, Schoeller H and Schon G 2000 *J. Low Temp. Phys.* **118** 391
Boese D, Hofstetter W and Schoeller H 2001 *Phys. Rev.* B **64** 125309
[36] Jarillo-Herrero P, Kong J, van der Zant H S J, Dekker C, Kouwenhoven L P and De Franceschi S 2005 *Nature* **434** 484
[37] Wilhelm U, Schmid J, Weis J and von Klitzing K 2002 *Physica* E **14** 385
[38] Holleitner A W, Chudnovskiy A, Pfannkuche D, Eberl K and Blick R H 2004 *Phys. Rev.* B **70** 075204
[39] Kogan A, Amasha S, Goldhaber-Gordon D, Granger G, Kastner M A and Shtrikman H 2004 *Phys. Rev. Lett.* **93** 166602

[40] Rosch A, Paaske J, Kroha J and Wolfle P 2003 *Phys. Rev. Lett.* **90** 076804
[41] Paaske J, Rosch A, Wolfle P, Mason N, Marcus C M and Nygard J 2006 *Nat. Phys.* **2** 460
[42] Pohjola T, Schoeller H and Schon G 2001 *Europhys. Lett.* **54** 241
[43] Lipinski S and Krychowski D 2005 *Phys. Status Solidi* b **243** 206
[44] Sun Q-f and Guo H 2002 *Phys. Rev.* B **66** 155308
[45] Holleitner A W, Blick R H, Huettel A K, Eberl K and Kotthaus J P 2002 *Science* **297** 70
[46] Kashcheyevs V, Schiller A, Aharony A and Entin-Wohlman O 2007 *Phys. Rev.* B **75** 115313
[47] Simon P, Cornaglia P S, Feinberg D and Balseiro C A 2007 *Phys. Rev.* B **75** 045310
[48] Świrkowicz R, Wilczyński M, Wawrzyniak M and Barnaś J 2006 *Phys. Rev.* B **73** 193312
[49] Meir Y, Wingreen N S and Lee P A 1993 *Phys. Rev. Lett.* **70** 2601
[50] Świrkowicz R, Barnaś J and Wilczyński M 2003 *Phys. Rev.* B **68** 195318
Świrkowicz R, Wilczyński M and Barnaś J 2006 *J. Phys.: Condens. Matter* **18** 2291
Krawiec M and Wysokiński K I 2002 *Phys. Rev.* B **66** 165408
[51] Lacroix C 1981 *J. Phys. F: Met. Phys.* **11** 2389